Overexpression and Functional Characterization of Kinin Receptors Reveal Subtype-Specific Phosphorylation[†,‡]

Andree Blaukat,[§,||,⊥] Kerstin Herzer,[§,||] Christian Schroeder,[§] Michael Bachmann,[§] Norman Nash,[#] and Werner Müller-Esterl*[,§]

Institute of Physiological Chemistry and Pathobiochemistry, University of Mainz, Duesbergweg 6, D-55099 Mainz, Germany, and Acadia Pharmaceuticals Incorporated, 3911 Sorrento Valley Boulevard, San Diego, California 92121

Received July 17, 1998; Revised Manuscript Received October 20, 1998

ABSTRACT: G protein-coupled receptors such as the receptors for bradykinin are present in low copy numbers in most natural cells. To overcome the problems associated with the analysis of these receptors at the protein level, we used highly efficient expression systems such as the baculovirus/insect cell system. However, the structural and functional statuses of recombinant receptors have often remained elusive. We have expressed the two types of human kinin receptors, B_1 and B_2, in Sf9 cells. Both receptors are found on the surface of infected cells where they display the same pharmacological profiles as their cognate receptors of native cells. The functional analysis of kinin receptors coupled to the intracellular signaling pathways of Sf9 cells revealed differential patterns of ligand-induced phosphorylation for the two kinin receptors. The B_1 receptor failed to undergo ligand-induced phosphorylation. However the B_2 receptor showed selective phosphorylation of a minor 38 kDa band and lack of phosphorylation of a dominant 33 kDa band, indicating that only a fraction of the receptor protein is functionally linked to the kinase pathway. A striking discrepancy between the number of binding sites and the amount of receptor protein per cell (molar ratio of 1:20 to 1:1000) indicated that a significant portion of kinin receptors is associated with the intracellular compartments of Sf9 cells. Pulse-chase and immunoprecipitation experiments demonstrated that the heterogeneity of recombinant receptors is not due to proteolytic processing but likely reflects incomplete or lacking N-glycosylation. We conclude that the baculovirus/Sf9 system is suitable for the recombinant expression and functional analysis of kinin receptors though limitations of the system have to be considered.

G protein-coupled receptors (GPCR)[1] are key components of the intercellular signaling networks which tune the homeostasis of multicellular organisms. Many of these GPCRs are functionally modulated by post-translational modifications such as phosphorylation, acylation, or glycosylation (*1*−*3*). For the understanding of the structural and functional implications of these modifications, studies of GPCRs at the protein level are indispensable. However, the amount of endogenous GPCRs present in primary cells (≤100 fmol/mg of cellular protein) or in cultured cells (10−10^3 fmol/mg) is often too low to allow the study of receptor modifications even though elaborate purification procedures and high-affinity antibodies for the receptors are available (*4*). Hence most of the information on GPCR proteins has been obtained with stably transfected CHO or HEK293 cells (expressing up to 5 pmol of receptor/mg of protein) and with transiently transfected COS cells (up to 20 pmol/mg) where the receptor genes are expressed under the control of strong viral promotors (*5*−*7*). By far the highest expression levels of GPCRs (up to 100 pmol/mg) have been obtained with the baculovirus/*Spodoptera frugiperda* system (*4, 8*−*14*). The benefits of this system are the ease of construction of recombinant virus, convenient culture conditions, high levels of recombinant protein, and low levels or even absence of endogenous receptors. On the downside, post-translational modifications of GPCRs are often incomplete in Sf9 cells (*9, 15*), and some of the major downstream signaling components such as G_i proteins are absent from Sf9 cells (*16*).

One prototypical group of GPCRs that is expressed in low copy numbers by native cells is the human kinin receptors. Kinins are peptide hormones mediating important biological processes such as hypotension, edema formation, pain sensation, smooth muscle contraction, and cell growth (*17*). The broad spectrum of their (patho)physiological activities

[†] This work was supported in part by grants from the Deutsche Forschungsgemeinschaft (MU 598/4-3) and from the Fonds der Chemischen Industrie (to W.M.E.).

[‡] This work forms part of the thesis of K.H.

* To whom correspondence should be addressed. Phone: +49−6131−395890. Fax: +49−6131−395793. E-mail: werner.muller-esterl@uni-mainz.de.

[§] University of Mainz.

[||] Both authors contributed equally to this study.

[⊥] Present address: Ludwig Institute for Cancer Research, Biomedical Center, Box 595, Husargatan 3, S-75124 Uppsala, Sweden.

[#] Acadia Pharmaceuticals Inc.

[1] Abbreviations: B_{max}, maximum number of binding sites; BSA, bovine serum albumin; ED, extracellular domain; FCS, fetal calf serum; FITC, fluorescein isothiocyanate; GPCR, G protein-coupled receptor; HMEM, minimum essential medium containing 20 mM Na^+-HEPES, pH 7.4; ID, intracellular domain; GST, bacterial glutathion-*S*-transferase; K_D, dissociation constant; KLH, keyhole limpet hemocyanin; MBP, bacterial maltose-binding protein; PAGE, polyacrylamide gel electrophoresis; PBS, phosphate-buffered saline; PVDF, polyvinylidenedifluoride; SDS, sodium dodecyl sulfate; TBS, 50 mM Tris, pH 7.5, 150 mM NaCl.

10.1021/bi981727r CCC: $18.00
Published on Web 01/05/1999

is mediated by cognate receptors which pharmacologically are classified as either B_1 or B_2 subtypes (*18*). B_2 receptors respond to bradykinin (Bk) and lysyl-Bk (kallidin) whereas their carboxy-terminally truncated variants, desArg^{9}bradykinin and desArg^{10}kallidin, stimulate B_1 receptors. The multiple biological effects elicited by the kinins are mediated by their intricate signaling pathways. Kinin receptors can couple to various G proteins such as $G\alpha_q$ $G\alpha_{13}$, $G\alpha_i$, or $G\alpha_s$ (*19*−*22*) and trigger diverse effector enzymes such as phospholipases A_2 and C_β (*23*), protein kinase C (*24*), and NO synthase (*25*). Many cells constitutively express the B_2 receptor at moderate levels while they express little if any B_1 receptor under basal conditions (*26, 27*). Even though inflammatory conditions upregulate the B_1 receptor biosynthesis, levels that would permit the analysis of the receptor protein are not reached. Therefore, the B_1 receptor, like numerous other GPCRs, has escaped classical attempts for purification or characterization at the protein level. Recombinant expression of the B_1 receptor in CHO cells has produced levels of 38 fmol/mg of protein (*28*); however, even under these conditions, specific antibodies to the receptor or to a fused tag failed to reveal B_1 protein (Blaukat, Faussner, and Müller-Esterl, unpublished experiments). Hence the molecular basis of the strikingly different desensitization patterns of B_1 and B_2 receptors (*28, 29*) has remained elusive.

Against this background we sought to recombinantly express kinin receptors in the baculovirus system and to analyze their ligand-binding capacity, their coupling to intracellular signaling pathways, and their protein-chemical features. Our study indicates that only a small fraction of the recombinant kinin receptors are functional; that is, they bind their cognate ligand with high affinity and trigger second messenger release, whereas the majority of the receptors resides in intracellular compartments. The portion of functional kinin receptors in Sf9 was sufficient to investigate their ligand-induced phosphorylation patterns. Our studies indicate that the differential desensitization patterns of kinin receptors likely reflect their divergent susceptibility to homologous phosphorylation.

EXPERIMENTAL PROCEDURES

Materials. Reagents were obtained from the following manufactures: Pro-mix [^{35}S] in vivo cell labeling mix (>1000 Ci/mmol) from Amersham; phosphate- and sulfur-free TC100 medium from Applichem; bradykinin, desArg^{10}-kallidin and desArg^{10}Leu^{9}kallidin from Bachem; Affigel 10 from BioRad; affinity-purified and preabsorbed antirabbit/mouse-IgG-F(ab′)$_2$ fragments coupled to horseradish peroxidase from Biotrend; DakoPen and fluorescein isothiocyanate (FITC)-labeled swine antirabbit immunglobulin from Dako; *N*-glycosidase F from Boehringer Mannheim; Nonidet P40 (NP-40) and Pansorbin from Calbiochem; HOE140 (D-Arginyl-arginyl-prolyl-4-hydroxyprolyl-glycyl-β-2-thienyl-alanyl-seryl-D-1,2,3,4-tetrahydroisoquinoline-3-carboxyl-[3aS,-7aS]-octahydro-indole-2-carboxyl-arginine-D-Arg^0-Hyp^3-Thi^5-D-Tic^7-Oic^8-bradykinin) from Hoechst (*30*); [^{32}P]H_3PO_4 (285 Ci/mg) from ICN; pVL-1392 and Liposom-Kit from Invitrogen; protein ladder marker (10−200 kDa) from Life Technologies Inc.; [2,3-prolyl-3,4-^{3}H]bradykinin (specific activity 98 Ci/mmol) and [^{3}H]dArg^{10}kallidin (specific activity Ci/mmol) from NEN DuPont; aprotinin, Pefabloc SC, Rotiquant, and scintillation cocktail Rotiszint eco plus from Roth; GF 52 glassfiber filters from Schleicher & Schuell; leupeptin, pepstatin A, and 1,10-phenanthroline from SERVA; and *N*-octylglycoside and polyethylenimine (50% (w/w) aqueous solution) from SIGMA. All other chemicals of analytical grade were from Applichem, Merck, or Roth.

Table 1: Synthetic Peptides and Recombinant Fusion Proteins Derived from the Sequences of the Human B_1 Receptor[a] and B_2 Receptor[b]

antigen[c]	domain[d]	positions	code
B_1 receptor			
ASS30	ED1	2−31	AS464
ELQ30	ED1	9−38	AS367
ENI17	ED2	95−111	AS373
SQD27	ID2	132−158	AS375
RSI30	ED3	176−205	AS369
SLR22	ID3	228−249	AS374
RLF29	ID4	317−343	AS370
KQC26	ID4	328−353	AS466
R76	ID4	338−353	AS530
MBP-SSW41	ED1	3−43	AS456
MBP-ISQ27	ID2	132−158	AS471
MBP-TFL32	ED3	171−202	AS474
MBP-FVG40	ID4	314−353	AS454
B_2 receptor			
CRS36	ID4	329−364	AS346
GST-Bk3/4	ED1	1−33	AS518
GST-Bk5/6	ED3	162−194	AS519
GST-Bk1/2	ID4	310−364	AS517

[a] Ref *31*. [b] Ref *32*. [c] MBP, maltose-binding protein; GST, glutathion-*S*-transferase. Unconjugated peptides were used for immunizations except for ENI-17 and SLR-22 which were previously coupled to keyhole limpet hemocyanin by 1-ethyl-3-(3-dimethylaminopropyl)-carbodiimide (*34*). Peptides are identified by their three amino-terminal residues using the one-letter code, followed by the total number of residues constituting the peptide. [d] ED, extracellular domain; ID, intracellular domain.

Cell Culture and Cloning of Baculoviruses. Sf9 cells from *S. frugiperda* were provided by Dr. H. Reiländer (Frankfurt, Germany) and grown in TC100 medium containing 10% (v/v) of fetal calf serum (FCS) and kept in air atmosphere at 27 °C. Recombinant baculoviruses were generated by cotransfection of Sf9 cells with the pVL1393 constructs containing the cDNA of the human B_1 receptor (*31*) or of the human B_2 receptor (*32*) and with linearized AcMVPV by the lipofection method (Invitrogen). Two days after lipofection, the supernatant was used to infect fresh Sf9 cells grown on 96-well plates at dilutions of 10^{-3}−10^{-6}, and positive viral clones were isolated. Subcloned recombinant viruses were identified by their capacity to direct protein expression as revealed by radioligand binding assay (see below). For protein expression Sf9 cells at 50−80% confluence were infected with recombinant baculovirus at a multiplicity of infection of 2−5 and harvested 36−72 h after infection.

Peptide Synthesis, Generation of Fusion Proteins, and Production of Antisera. Peptides derived from the various intracellular domains (ID) ID2−ID4 and extracellular domains (ED) ED1−ED3 of the human B_1 receptor sequence were synthesized by the solid phase method using fluorenylmethyloxycarbonyl (Fmoc) chemistry (Table 1). The peptides were used for immunization without prior conjugation to carrier protein except for ENI-17 and SLR-22 which were previously coupled to keyhole limpet hemocyanin (KLH) by 1-ethyl-3-(3-dimethylaminopropyl)-carbodiimide (*34*). Bacterial fusion proteins of B_1 or B_2 receptor sequences

(see Table 1) were generated according to the manufacturer's instructions using maltose-binding protein (MBP) constructs (Biolabs) or glutathione-*S*-transferase (GST) constructs (Pharmacia). Female New Zealand White rabbits were immunized using standard procedures. The production and characterization of antipeptide antibodies to the B_2 receptor are detailed elsewhere (*33*, *34*). Some antibodies were affinity-purified utilizing the cognate antigen covalently coupled (5 mg of peptide/mL of matrix) to affigel 10 (*35*). A reference antibody directed to the carboxy-terminal domain ID4 (R76, AS520) of the human B_1 receptor was kindly provided by Dr. J. F. Hess, Merck Inc., Rahway, N. J. (*36*).

Radioligand-Binding Studies. The binding activity of B_1 and B_2 receptors was assayed in cell suspensions using [^{3}H]dArg^{10}kallidin and [^{3}H]bradykinin, respectively. At varying periods after infection of Sf9 cells the medium was aspirated, and the cells were carefully rinsed 2 times with ice-cold serum-free TC100 medium containing 0.5% (w/w) bovine serum albumin (BSA) and 2 mM bacitracin. Following resuspension in the same medium 10^5 cells were incubated under gentle agitation with a saturating concentration of 5 nM radioligand in the absence (total binding) or in the presence (nonspecific binding) of 5 μM unlabeled kinin at 4 °C. After 90 min (i.e., equilibrium conditions) the unbound ligand was removed by rapid filtration through GF 52 glassfiber filters pretreated with 0.3% (m/v) polyethylenimine for 15 min. After 4 washes with 4 mL each of ice-cold 14% (v/v) 2-propanol, scintillation cocktail (4 mL of Rotiszint eco plus) was added to the dried filters and bound radioactivity was measured. Dissociation constants (K_D) for cell-surface-exposed receptors (B_{max}) were calculated by Scatchard analysis with radioligand concentrations ranging from 10 pM to 10 nM. For the determination of total cellular protein, 10^5 cells were lysed in 1 M NaOH and assayed with Rotiquant solution according to the manufacturer's protocol using BSA as the standard protein.

Measurement of Changes in Intracellular Free [Ca^{2+}]. Intracellular free Ca^{2+} concentrations, $[Ca^{2+}]_i$, in Sf9 cells were determined using the fluorescence dye fura-2/AM as described (*37*). Briefly 24−42 h after infection 10^5 cells were collected, washed 2 times with minimum essential medium (MEM) buffered with 20 mM Na^+-HEPES, pH 7.4 (HMEM), resuspended in the same medium, and incubated for 45 min at 30 °C under gentle agitation with 2 μM fura-2/AM in HMEM containing 0.04% (m/v) pluronic F-127. The cells were sedimented, washed 2 times as above, and incubated in HMEM for another 30 min to allow for complete deesterification of fura-2/AM. The cell suspensions were placed into thermostated cuvettes, and the fluorescence at 510 nm was measured. The excitation wavelength was alternated between 340 and 380 nm in intervals of 600 ms. Changes in $[Ca^{2+}]_i$ are given as the ratio of intensities at 340 and 380 nm, respectively.

Immunoblotting. Sf9 cells expressing the human kinin receptors were washed 2 times with 50 mM tris(hydroxymethyl)aminomethane (Tris), pH 7.5, 150 mM NaCl (TBS) and lysed in sample buffer (65 mM Tris-HCl, pH 6.8, 5% (m/v) sodium dodecyl sulfate (SDS), 6 M urea, 25 mM dithiothreitol, 0.05% (m/v) bromophenol blue) for 30 min at 42 °C. Proteins (1−10 μg/p lane) were separated by 10% SDS−polyacrylamide gel electrophoresis (PAGE) and transferred on poly(vinylidene difluoride) (PVDF) membranes by semi-dry blotting for 45 min at 1.5 mA/cm^2 using 39 mM Tris, 48 mM glycine, 1.3 mM SDS. Membranes were blocked with 5% (m/v) fat-free milkpowder in TBS with 0.1% (m/v) NP-40 (blocking buffer) and incubated with antiserum diluted 1:500 to 1:2000 in the same buffer or with 0.5−5 μg/mL affinity-purified antibody. For protein visualization, antirabbit-IgG-F(ab′)$_2$ coupled to horseradish peroxidase was diluted 1:5000 in blocking buffer, followed by the chemiluminescence detection method. To estimate the detection limits of the method, we separated serial dilutions of bacterial fusion proteins containing the relevant sequences by SDS−PAGE, applied antipeptide antibodies, and analyzed the intensities of the resultant bands with the Photoshop 4.0 program.

[^{35}S]-Labeling and Immunoprecipitation. At varying times after infection, Sf9 cells on 6-well dishes were washed 2x with sulfur-free TC100, incubated for 30 min at 27 °C in the same medium, and labeled with 0.1 mCi/mL [^{35}S]-methionine/cysteine (Pro-mix) for 3 h. After 3 washes with TBS, the cells were lysed with 1% (m/v) NP-40, 0.5% (m/v) deoxycholate, 0.1% (m/v) SDS in TBS including protease inhibitors (10 μg/mL each of leupeptin, aprotinin, pepstatin A and 1,10-phenanthroline, and 1 mM Pefabloc) (lysis buffer) and receptors were immunoprecipitated with 2.5 μL of antiserum or 1−10 μg of affinity-purified antibodies as described (*33*). For control preimmune serum or preabsorbed serum (probe) and wild-type, baculovirus-infected or noninfected cells (antigen) were used. For enzymatic deglycosylation the immunoprecipitated [^{35}S]-labeled proteins were incubated with 2 units of *N*-glycosidase F in 20 μL of 50 mM NaH_2PO_4, pH 7.5, 0.1% (m/v) *N*-octylglycoside. After 12 h at 30 °C the reaction was stopped with 20 ?l of sample buffer, proteins were separated by reducing 10% SDS−PAGE and were visualized by fluorography using 15% (m/m) sodium salicylate as the fluorophor.

Quantification of Immunoblots and Autoradiographs. Western blots were scanned by an AGFA StudioStar using the Fotolook SA 2.09.1 program imported into Photoshop 4.0. Settings of scanner and programs were kept constant throughout the measurements. Areas containing proteins bands of interest were marked, and the corresponding histograms were displayed in the image menu to indicate the number of pixels at each brightness level. The mean intensity value calculated by the program represents the average brightness of the selected area and serves as a measure for band intensity. The results obtained by this method were in good agreement with those made by phosphoimaging.

Receptor Phosphorylation. Sf9 cells grown on 6-well dishes and infected with recombinant baculoviruses for 36−40 h were washed 2 times with phosphate-free TC100 medium. After incubation for 1 h at 27 °C in the same medium, cells were labeled with 0.25 mCi/mL [^{32}P]orthophosphate for 3 h. The cells were exposed for 10 min to 100 nM bradykinin or dArg^{10}kallidin alone or in combination with 1 μM competing antagonist dArg^{10}Leu^{9}kallidin (B_1) or 1 μM HOE140 (B_2) at 27 °C, washed 3 times with TBS buffer, and scraped into 1 mL of ice-cold lysis buffer including phosphatase inhibitors (50 mM sodium fluoride, 1 mM sodium orthovanadate, 25 mM sodium pyrophosphate). Solubilization and immunoprecipitation were done as previously detailed (*33*). The resultant precipitates were

analyzed by 10% SDS−PAGE and autoradiography. A GS-250 Molecular Imager (BioRad) was used for quantitative analysis of incorporated [^{32}P]phosphate.

Immunofluorescence Analysis. Sf9 cells were infected with recombinant baculovirus for 30 h; thereafter cells tended to disintegrate. The cells were washed 3 times with 6.5 mM Na_2HPO_4, 1.5 mM KH_2PO_4, 2.7 mM KCl, 137 mM NaCl, pH 7.4 (PBS), fixed with 3% (v/v) paraformaldehyde in PBS for 15 min, and washed 3 times with PBS. A fraction of the cells was permeabilized with ice-cold methanol for 15 min at 4 °C and then washed 3 times with PBS containing 0.5% (m/v) BSA. Cells incubated for 30 min at 37 °C in a humidified atmosphere with the relevant antiserum diluted 1:500 in PBS containing 0.5% BSA. After 3 washes with PBS/0.5% BSA the cells were incubated with a FITC-conjugated antirabbit immunoglobulin developed in swine (1:5000) for 30 min at 37 °C in a humidified atmosphere. Stained cells were washed 3 times with PBS containing 0.5% BSA and mounted with MOVIOL. Preimmune serum, omission of the first antibody, or noninfected cells were used as the controls. Serial optical sections at a z-distance of 5 μm were prepared and stored. Labeled cells were analyzed using a Zeiss confocal laser scanning microscope (LSM 10).

RESULTS

Kinin-Binding Sites Expressed by Infected Sf9 Cells. To follow the time course of kinin receptor expression in intact Sf9 cells, we performed binding assays at saturating concentrations of 5 nM [^{3}H]desArg^{10}kallidin (B_1) or 5 nM [^{3}H]-bradykinin (B_2) under equilibrium conditions. Specific [^{3}H]desArg^{10}kallidin binding indicative of the recombinant B_1 receptor first occurred 36 h after infection (Figure 1A), whereas noninfected Sf9 cells or cells infected with an irrelevant virus construct failed to produce significant binding (data not shown). Expression of B_1-binding sites sharply increased after 60 h and reached a maximum at 84 h. At maximum expression the dissociation constant (K_D) for desArg^{10}kallidin was 0.5 nM, and the maximum number of binding sites (B_{max}) was 150 fmol/mg of cell protein. Similarly, [^{3}H]bradykinin-binding sites indicating the B_2 receptor appeared 36 h after infection, followed by a rapid increase over the next 24 h (Figure 2A). Thereafter expression of bradykinin-binding sites leveled off (60−84 h). Scatchard analysis of cells harvested at 72 h revealed a K_D of 2 nM for bradykinin and a B_{max} of approximately 2000 fmol/mg of protein. Competition binding studies using standard kinin receptor agonists and antagonists indicated that the pharmacological profiles of the recombinant kinin receptors from Sf9 cells were indistinguishable from those obtained with native mammalian cells (data not shown).

Immunoprint Analysis of Recombinant Kinin Receptors. We sought to correlate the appearance of kinin-binding sites with the emergence of kinin receptor protein. To this end we generated a panel of antibodies against synthetic peptides and/or fusion proteins covering most of the predicted intra- and extracellular domains of the B_1 receptor (Table 1). The antisera were strongly positive for their respective antigen in the indirect ELISA (data not shown), and most of them recognized the recombinant B_1 receptor in Western blots. For example, affinity-purified antibodies to the amino-terminal extracellur domain-1 (ED1) of the B_1 receptor

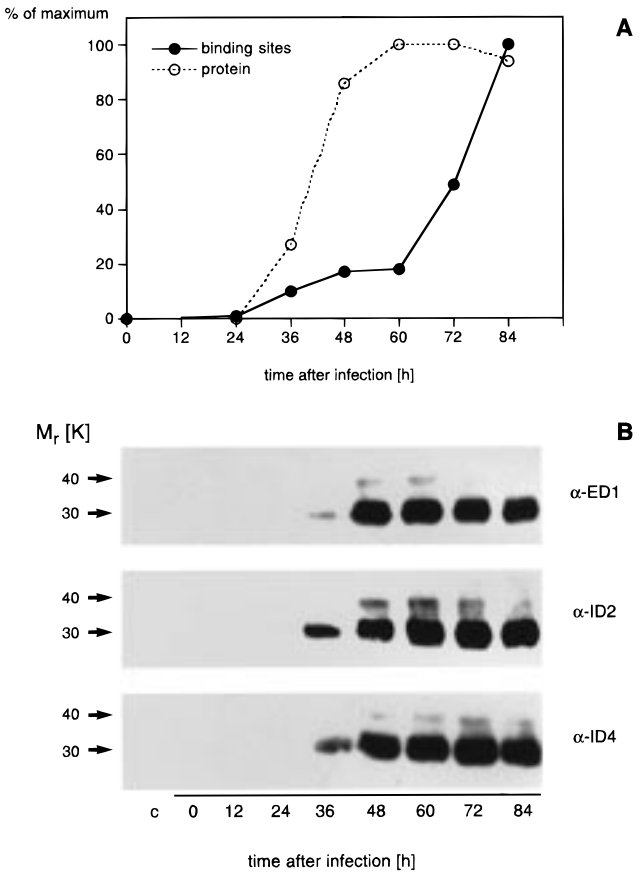

FIGURE 1: Expression of kinin B_1 receptor in Sf9 cells. A baculovirus construct encompassing the full-length human B_1 receptor cDNA was used to infect Sf9 cells. Aliquots (~10^5 cells) were harvested at the indicated time points after infection. (A) Cells were analyzed for specific [^{3}H]desArg^{10}kallidin (5 nM) binding at 4 °C for 90 min (filled circles, straight line). Results are means of three independent experiments and are given as the percentage of maximum binding at 84 h (B_{max} = 150 fmol/mg). B_1 protein was quantified by scanning the immunoblots presented in panel B using Photoshop 4.0 (open circles, dotted line). Results are means of three experiments using distinct antibodies. (B) Cells (~10^5) were lysed in sample buffer, and 10 μg of total protein each was analyzed by reducing 10% SDS−PAGE. Following transfer to PVDF sheets protein was visualized with 0.5−5 μg/mL affinity-purified antibodies to B_1 receptor domains ED1 (α-ED1; AS367), ID2 (α-ID2; AS375), or ID4 (α-ID4; AS520). Control ("C") was done with cells infected by an unrelated baculovirus. Relative molecular masses of standard proteins are indicated (left).

produced a band of 30 ± 3 kDa when Sf9 cells were collected 36 h after infection (Figure 1B, top panel). The intensity of the major 30 kDa band acutely increased over the next 12 h and reached a maximum at 60−84 h after infection. Prolonged exposure revealed additional faint bands at 40 ± 4 and 60 ± 6 kDa (not shown in Figure 1B). Similar profiles were generated with antibodies to intracellular domain ID2 (Figure 1B, center) or to carboxy-terminal domain ID4 (lower panel) of the B_1 receptor. The kinetics of appearance of desArg^{10}kallidin-binding sites and of B_1 receptor protein were grossly divergent (Figure 1A), suggesting that only a fraction of the de novo synthesized B_1 receptors immediately acquire ligand-binding capacity. Similar results were obtained when lower loading levels of receptor protein were used.

For the B_2 receptor we used previously characterized antisera to synthetic peptides (*33*) or fusion proteins derived from the human receptor sequence. An antibody to ED1

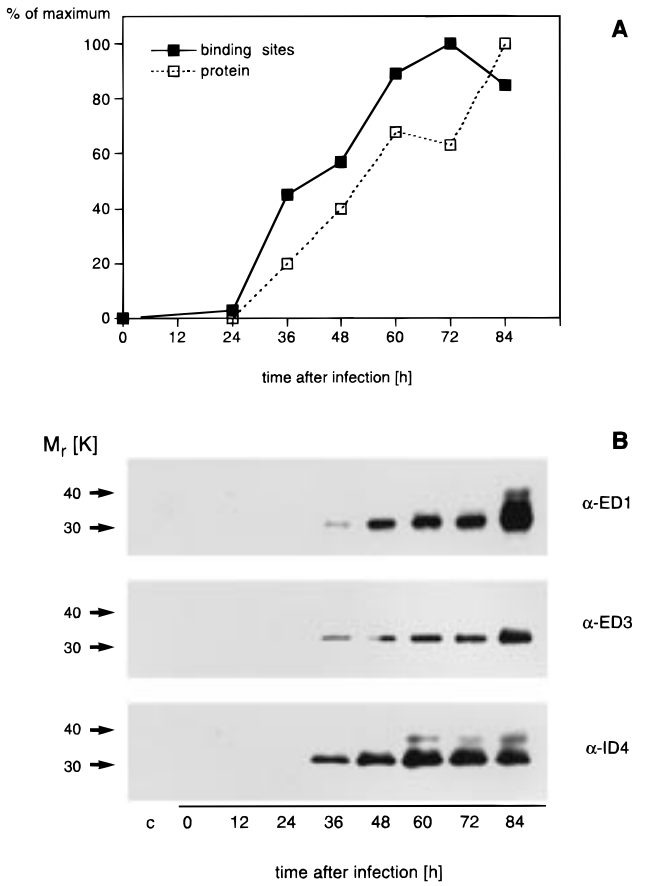

FIGURE 2: Expression of kinin B_2 receptor in Sf9 cells. A baculovirus construct encompassing the entire human B_2 receptor cDNA was used to infect Sf9 cells. Cells ($\sim 10^5$) were harvested at the indicated time points after infection. (A) Cells were analyzed for specific [^{3}H]bradykinin (5 nM) binding at 4 °C for 90 min (filled squares, straight line). Results are means of three independent experiments and are given as the percentage of maximum binding at 72 h (B_{max} = 2 pmol/mg). B_2 protein was quantified by scanning of the immunoblots presented in panel B using Photoshop 4.0 (open squares, dotted line). Results are means of three experiments using distinct antibodies. (B) Aliquots ($\sim 10^5$ cells) were lysed in sample buffer, and 10 μg of total protein each was analyzed by reducing 10% SDS−PAGE. Following transfer to PVDF sheets protein was visualized with antisera (1:1000) to B_2 receptor domains ED1 (α-ED1; AS518), ED3 (α-ED3; AS519), or ID4 (α-ID4; AS346). Control ("C") was done with cells infected by an unrelated baculovirus.

stained for a 33 ± 3 kDa protein that was first visible 36 h after infection (Figure 2B). Upon prolonged exposure additional faint bands of 38 ± 4 kDa and 70 ± 7 kDa appeared (not shown in Figure 2B). The intensity of the major 33 kDa band increased over the next 24 h and leveled off at 60−84 h. Antibodies to ED3 (Figure 2B, center panel) or to ID4 (lower panel) of the B_2 receptor produced similar though not identical immunoprinting patterns; the reasons for the observed variability in the staining patterns are unknown. Together these data suggest that the kinetics of appearance of binding sites and receptor protein seem to concur for the B_2 receptor.

Quantification of Immunoprints. To follow the time courses of receptor protein appearance more accurately, we sought to quantify the corresponding immunoprints. To this end we purified bacterial fusion proteins comprising MBP and the domain ID4 of the B_1 receptor or GST and ID4 of the B_2 receptor and subjected them to SDS−PAGE and

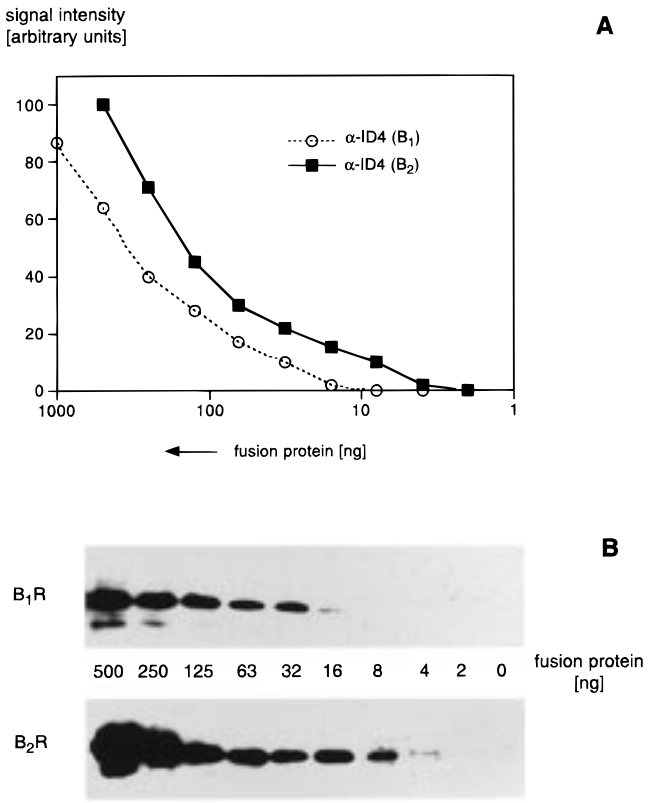

FIGURE 3: Sensitivity of antipeptide antibodies to kinin receptors. Fusion proteins of MBP and the carboxy-terminal domain ID4 of the B_1 receptor or GST and ID4 of the B_2 receptor were expressed in *Escherichia coli*, purified to apparent homogeneity, and applied (2−500 ng) to reducing 10% SDS−PAGE. Following transfer to PVDF sheets the receptor proteins were probed by antipeptide antisera to ID4 (α-ID4), that is, AS520 for B_1 or AS346 (B_2), at a dilution of 1:1000 each and visualized by the chemiluminescence method. (A) The immunoblotted B_1 protein (open circles, dotted line) or B_2 protein (filled squares, straight line) was quantitated by scanning the blots presented in panel B using Photoshop 4.0. (B) Immunoblots of 2−500 ng of kinin receptor fusion constructs. A representative of 3 independent experiments is shown. For the B_1 receptor an extra experiment was done with 1 μg of the fusion protein (not shown).

Western blotting using antipeptide antibodies to the cognate receptor domains. Application of 2−500 ng of fusion protein allowed us to establish calibration curves for the two receptor constructs (Figure 3A). A minimum amount of 16 ng ($\sim$350 fmol) of B_1 fusion protein was readily detectable under these conditions, whereas the lower detection limit for the B_2 construct was 4 ng ($\sim$120 fmol). Controls with GST or MBP alone were negative as were cross-controls for the antibodies, that is, anti-B_2 for the B_1 receptor and vice versa (not shown). The sensitivity of anti-B_2 appeared to be 3−10-fold higher over the entire mass range compared to anti-B_1 (Figure 3A). Taking advantage of these calibration curves we re-examined the receptor bands in the immunoprints of Figures 1 and 2. Semiquantitative analysis indicated that at maximum expression levels approximately 30−100 pmol of B_1 per mg of cellular protein and 40−200 pmol/mg of B_2 receptor were present in Sf9 cells. The variability was due to different antibodies used as the probes (cf. Figures 1 and 2, bottom panels). Comparing these data with the amount of receptor judged from functional binding assays we found a 200−1000-fold molar excess of B_1 protein over desArg^{10}kallidin-binding sites, and a 20−100-fold molar excess of B_2 protein

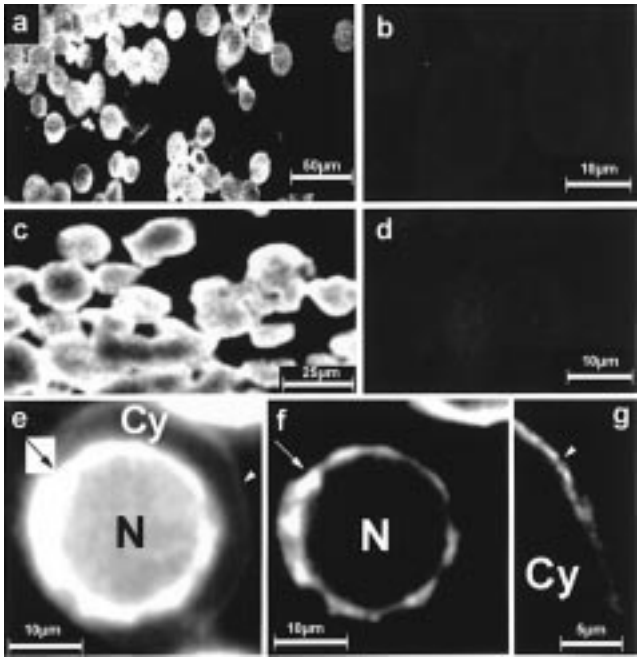

FIGURE 4: Confocal laser scanning microscopical analysis of kinin receptors in Sf9 cells. Sf9 cells infected for 30 h with competent baculovirus encoding the B_1 receptor (a,b) or the B_2 receptor (c−g) were fixed and permeabilized. Antisera AS464 to ED1 of the B_1 receptor (a) and AS518 to ED1 of the B_2 receptor (c, e−g) were applied at 1:500 dilutions in PBS/0.5% BSA, and bound antibodies were probed with a FITC-labeled swine antirabbit immunglobulin at 1:5000. Preimmune sera were used for controls (b, d).

over bradykinin-binding sites. These findings disclose that only a minute fraction of the total receptor protein, that is, ≤0.5% of the B_1 receptor and ≤5% of the B_2 receptor, acquires ligand-binding capability and hence signaling activity. Because our ligand-binding assays detect only surface-exposed binding sites, we cannot exclude at this point that a large proportion of the newly synthesized receptor protein is retained in intracellular compartments, probably due to incomplete processing or misrouting, and therefore it is not accessible by externally applied radioligand probes.

Epifluorescence and Confocal Laser Scanning Microscopy of Kinin Receptors. To test the hypothesis that a major portion of the total receptor protein resides within Sf9 cells, we studied the cellular distribution of B_1 and B_2 receptors using epifluorescence and confocal laser scanning microscopy. As expected antibodies to the respective amino-terminal receptor domains revealed a positive staining of cells infected by the recombinant baculovirus for the B_1 receptor (Figure 4a) and the B_2 receptor (Figure 4c) while controls with the corresponding preimmune serum were negative (Figure 4b,d). Stained cells were cut into optical sections by confocal microscopy (exemplified for the B_2 receptor in Figure 4e−g). Mounted stacks of optical sections (Figure 4e) and a single optical section taken at the z-distance of 10 μm from the bottom (Figure 4f) displayed an intensely stained rim surrounding the nucleus that most likely represents the endoplasmic reticulum/Golgi region (arrows in Figure 4e,f). However, a diffuse staining of the plasma membrane was seen (arrowhead in Figure 4e). Focusing and optimizing the signal level highlighted the immunostaining of the cell surface (Figure 4g). Collectively these findings suggest that the vast majority of immunoreactive kinin receptor protein is retained in intracellular compartments of

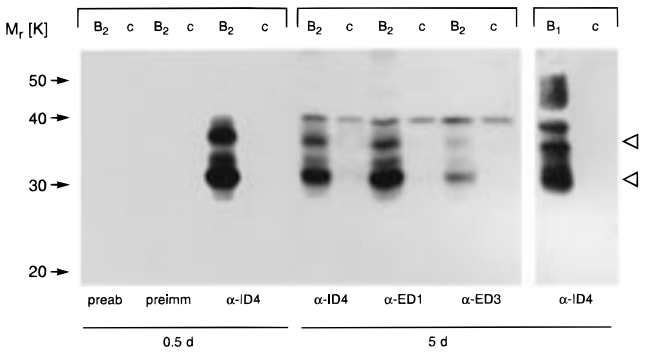

FIGURE 5: Immunoprecipitation of [^{35}S]-labeled kinin receptors. Sf9 cells were infected for 48−60 h with baculovirus encoding the human B_1 receptor (right panel) or the human B_2 receptor (left panel). Cells were labeled with 0.1 mCi/mL [^{35}S]methionine/cysteine for 3 h prior to harvesting and cell lysis. Solubilized cellular protein was immunoprecipitated with 2.5 μL each of antiserum to domain ID4 (α-ID4; AS520) of the B_1 receptor (right panel), antiserum to peptide CRS36 (α-ID4; AS346) of the B_2 receptor (left panel), or antisera to fusion proteins of various domains, α-ID4 (AS517), α-ED1 (AS518), or α-ED3 (AS519), of the B_2 receptor (center panel). Immunopreciptates were analyzed by reducing 10% SDS−PAGE and fluorography; varying exposure times are indicated (bottom). Cells infected with an irrelevant baculovirus served as a control ("C"). Antiserum specificity was probed by preimmune serum ("preimm") and immune serum that had been preabsorbed on the authentic antigen, peptide CRS36 ("preab"). Open arrowheads point to the major translation products. For details of the antigens and antisera, see Table 1.

infected Sf9 cells, with a small fraction of receptors reaching the cell surface.

Immunoprecipitation of [^{35}S]-Labeled Kinin Receptors. In an effort to examine the recombinant kinin receptors more closely at the protein level, we developed antibody probes that would allow the immunoprecipitation of radiolabeled kinin receptors from infected insect cells. To this end we screened a panel of antibodies to synthetic peptides and fusion proteins for their capacity to immunoprecipitate [^{35}S]-labeled kinin receptors from total cellular lysates. Sf9 cells shortly before maximum receptor expression (cf. Figures 1 and 2) were metabolically labeled with 0.1 mCi/mL [^{35}S]-methionine/cysteine for 3 h. Following solubilization the receptors were immunoprecipitated and analyzed by 10% SDS−PAGE and fluorography (Figure 5). An antipeptide antibody directed to intracellular domain ID4 (α-ID4) efficiently precipitated B_2 protein from Sf9 cells that had been infected with the cognate baculovirus but not from cells infected with the wild-type virus. Consistent with the results from Western blotting, a strong band of 33 ± 3 kDa, a weaker band of 38 ± 4 kDa, and a very faint band of 70 ± 7 kDa were seen. Controls with the preabsorbed antiserum or the corresponding preimmune serum were negative (Figure 5, left panel). Similar band patterns were seen with antibodies directed against GST fusion proteins expressing ED1, ED3, or ID4 of the B_2 receptor (Figure 5, center panel). For the antibodies to fusion proteins, prolonged exposure times of 5 days had to be applied while 0.5 days was sufficient for antipeptide antibodies (Figure 5, center vs left panel). For the B_1 receptor, an antiserum directed to a peptide of intracellular domain ID4 (α-ID4) revealed major bands between 30 and 50 kDa for infected cells but not for controls (Figure 5, right panel). Other antisera listed in Table 1 worked poorly, and some even failed to precipitate significant amounts of the B_1 receptor (not shown). Hence, for both types of kinin

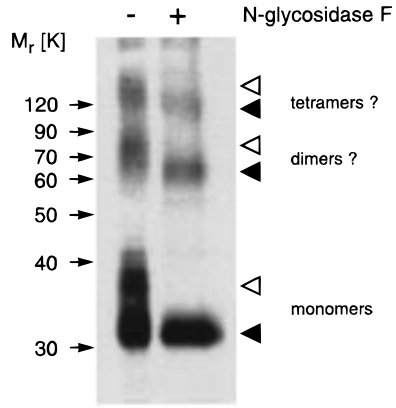

FIGURE 6: Enzymatic deglycosylation of [^{35}S]-labeled B_2 receptor. [^{35}S]-Labeled B_2 receptor protein was immunoprecipitated with antiserum AS346 (α-ID4) from Sf9 cells infected with a competent virus. The precipitated receptor was redissolved in 20 μL of 50 mM NaH_2PO_4, pH 7.5, 0.1% (m/v) *N*-octylglycoside and incubated for 12 h at 30 °C in the presence (+) or absence (−) of 2 units of N-glycosidase F. The reaction was stopped by adding 20 μL of reducing sample buffer. Proteins were resolved by 10% SDS−PAGE and visualized by fluorography. Arrowheads point to the major products before (open) and after (closed) deglycosylation.

receptors antipeptide antibodies to their carboxy-terminal domains proved most suitable for immunoprecipitation.

Enzymatic Deglycosylation of B_2 Receptor. Since, the immunoprecipitated kinin receptors showed a marked heterogeneity, and because the size of their major bands (∼30 kDa) were well below the molecular masses predicted from their corresponding cDNAs (∼40 kDa) or those found in native cells (∼70 kDa for the B_2 receptor) (*33*, *34*, *38*, *39*), we wondered whether these findings were solely due to the overall hydrophobicity of recombinant receptors (*9*), or whether they reflected incomplete glycosylation and/or proteolytic processing of the primary translation products. Since antibodies to the extreme amino- and carboxy-terminal segments recognize the receptor proteins (cf. Figures 1, 2, and 5), we considered proteolytic degradation of the receptors unlikely. To address the carbohydrate processing we chose to enzymatically deglycosylate the immunoprecipitated B_2 receptor in vitro. B_2 receptor was precipitated from lysate of Sf9 cells that had been labeled for 3 h with [^{35}S]amino acids, after maximum expression. The immunoprecipitated proteins were dissolved in phosphate buffer containing 0.1% *N*-octylglucoside and incubated for 12 h at 30 °C in the absence (control) or presence of 2 units of *N*-glycosidase F. The reaction products were then analyzed by SDS−PAGE and fluorography (Figure 6). As expected the untreated sample showed a major band 33 ± 3 kDa and a minor band 38 ± 4 kDa. Faint broad bands of 70 ± 7 and 140 ± 14 kDa were also visible. The glycosidase-treated sample still showed a major 33 kDa band. However, the 38 kDa band was absent, and the high molecular mass bands had shifted down to 65 ± 6 and 120 ± 12 kDa, respectively. These results suggest that the 33 kDa protein represents the full-length nonglycosylated receptor with an unusual migration behavior in SDS−PAGE, while the 38 kDa protein typifies a partially glycosylated receptor that likely forms oligomers of 70 kDa (dimer) and 140 kDa (tetramers). The 33 kDa precursor does not appear to form a dimer of approximately 66 kDa (cf. Figure 6, left lane), suggesting that only the processed form(s) of the B_2 receptor oligomerizes, probably

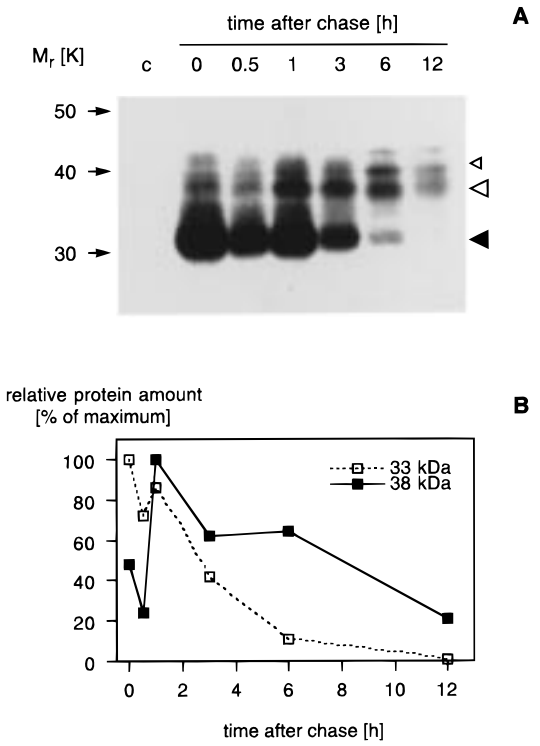

FIGURE 7: Pulse-chase of B_2 receptor translation products. Sf9 cells infected with a competent baculovirus were incubated with 0.5 mCi/mL [^{35}S]methionine/cysteine for 30 min (pulse). The cells were washed, and fresh medium containing an excess of unlabeled amino acids was added (chase). Aliquots of the cells were lysed after 0−12 h of chase, and the B_2 receptor was immunoprecipitated with antiserum AS346 (α-ID4). (A) Immunoprecipitates were analyzed by reducing 10% SDS−PAGE and fluorography. The arrowheads (right) point to the major translation products of 33 kDa (large open arrowhead), 38 kDa (closed), and 42 kDa (small), respectively. (B) The 33 kDa protein (open squares, dotted line) and the 38 kDa protein (filled squares, straight line) were quantified using an imaging system (GS-250, BioRad). Data are means of three independent experiments and are given as the percentage of maximum level at $t = 0$ h (33 kDa protein) and $t = 1$ h (38 kDa protein), respectively.

after translocation from the endoplasmic reticulum to the cell surface (see below). Because the band pattern of Figure 5 clearly suggests multiple glycosylation of the B_1 receptor from Sf9 cells, we applied the identical deglycosylation procedure. Unlike for the B_2 receptor we did not observe significant amounts of deglycosylated B_1 receptor; the reasons for this failure are unknown.

Pulse-Chase Experiments. Because the 33 kDa nonglycosylated B_2 receptor is the dominant band in Western blots and immunoprecipitates, we speculated that it may represent the precursor to the minor 38 kDa band. To test this hypothesis we performed pulse-chase experiments. Infected Sf9 cells at maximum expression levels were incubated with 0.5 mCi/mL [^{35}S]amino acids for 30 min (pulse). The cells were washed, and fresh medium containing a molar excess of unlabeled amino acids was added (chase). After 0−12 h of chase aliquots of the cell culture were removed, cells were lysed, and the B_2 receptor protein was immunoprecipitated and analyzed by SDS−PAGE. At $t = 0$ the 33 kDa band was paramount; over the next 6 h of chase it gradually faded, and after 12 h it was completely gone (Figure 7A). By marked contrast the 38 kDa protein was faint at $t = 0$ h and increased until 1 h of chase; thereafter the intensity of the

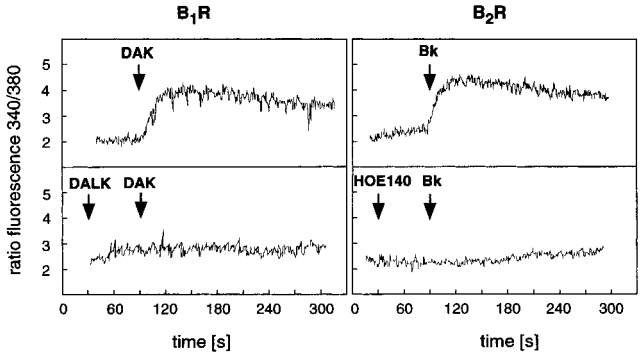

FIGURE 8: Kinin-induced Ca^{2+} transients in infected Sf9 cells. Sf9 cells expressing the human B_1 receptor (left panels) or the human B_2 receptor (right panel) were stimulated with 1 nM desArg[10]kallidin (DAK) or 1 nM bradykinin (Bk), and the intracellular calcium concentration $[Ca^{2+}]_i$ was followed as the change in the ratio of fura-2 fluorescence at 340/380 nm (top panels). For control the cells were preincubated for 1 min with 10 nM corresponding antagonist, desArg[10]Leu[9]kallidin (DALK) or HOE140 (bottom panels).

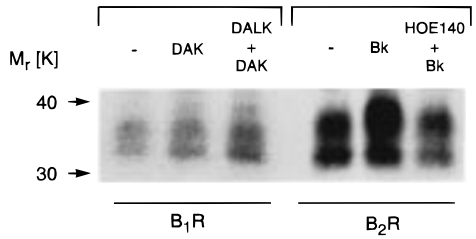

FIGURE 9: Ligand-induced phosphorylation of kinin receptors. Sf9 cells were infected for 42−60 h with competent baculoviruses for the B_1 (left panel) or B_2 receptor (right panel), and then labeled with 0.25 mCi/ml [^{32}P]orthophosphate for 3 h. Cells were stimulated for 10 min with desArg[10]kallidin (DAK) or bradykinin (Bk) alone or in combination with 1 μM competing antagonists desArg[10]Leu[9]-kallidin (DALK; B_1) or HOE140 (B_2). Controls were done in the absence of a ligand (−). Following lysis and solubilization the kinin receptors were immunoprecipitated with antisera to ID4, AS520 (B_1), or AS346 (B_2). The immunoprecipitates were analyzed by reducing 10% SDS−PAGE and autoradiography, and quantified by Photoshop or a phosphoimager. A representative of 3 independent experiments is shown.

band moderately declined, and it was still present after 12 h of chase. Yet another band of 42 kDa displayed a similar time course though its peaking was delayed until 6 h of chase. Semiquantitative analysis of the incorporated radioactivity revealed that the half-lives of the 33 and 38 kDa species are 2.5 and 8 h, respectively (Figure 7B). The findings are compatible with the conclusion that the 33 kDa band is a primary translation product which is converted into a 38 kDa protein, most likely by post-translational modification such as glycosylation. Given the predominance of the 33 kDa precursor in various assays of Sf9 cells, one is tempted to speculate that it may represent the immature, that is, nonfunctional, form of the B_2 receptor whereas the 38 kDa and/or 42 kDa proteins could typify functional receptor forms. Our notion that the 33 kDa protein may represent the primary translation product, that is, the full-length form of the receptor, is strongly supported by the finding that the 33 kDa band cross-reacts with antibodies directed to epitopes located at the extreme NH_2- and COOH-terminal regions of the receptor (cf. Figures 2 and 5).

Functional Coupling of Kinin Receptors in Sf9 Cells. To further the characterization of the recombinant receptor proteins and to eventually determine the functional entity, we addressed the signaling properties of kinin receptors in Sf9 cells. We loaded infected cells with the Ca^{2+}-sensitive fluorescence dye fura-2, challenged the cells with 1 nM desArg[10]kallidin (B_1) or bradykinin (B_2), and followed the change of the intracellular Ca^{2+} concentration, $[Ca^{2+}]_i$. Stimulation of Sf9 cells bearing B_1 or B_2 receptors induced a transient rise in $[Ca^{2+}]_i$ (Figure 8, upper panels). Preincubation of the cells with 10 nM of an antagonist, that is, Leu[9]-dArg[10]kallidin (B_1) or HOE140 (B_2) abrogated the agonist-induced rise in $[Ca^{2+}]_i$ (Figure 8, lower panels). Also stimulation of noninfected cells or of cells infected with an irrelevant virus did not result in a Ca^{2+} flux (not shown). The appearance of functional receptor, that is, ligand-promoted Ca^{2+} increase, coincides with the upregulation of receptor protein after 24 h of infection (not shown). Together these findings demonstrate that at least a fraction of recombinant kinin receptors couples to the Ca^{2+} signaling pathway of Sf9 cells, presumably through G_q-mediated cascades. Thus it appears that the Sf9 expression system allows the functional analysis of kinin receptors in an appropriate cellular context.

Ligand-Induced Phosphorylation of Kinin Receptors in Sf9 Cells. We have previously demonstrated that ligand-induced phosphorylation induces a swift desensitization of the B_2 receptor (*33*). Others have shown that ligand stimulation of the B_1 receptor triggers a long-lived signaling activity without apparent desensitization (*28, 29*). The reasons for the differential desensitization patterns of kinin receptors have remained unknown. To address this issue and to identify the receptor form(s) phosphorylated in response to kinins, we labeled infected Sf9 cells with [^{32}P]orthophosphate and stimulated them with 100 nM desArg[10]kallidin (B_1) or bradykinin (B_2). Following immunoprecipitation the intrinsically labeled proteins were resolved by SDS−PAGE and analyzed by autoradiography. Bradykinin induced a 2.0 ± 0.5-fold to 3.1 ± 0.6-fold increase of phosphorylation of the B_2 receptor (Figure 9, right panel). Incorporation of radiolabeled phosphate was completely blocked by preincubation of the cells with 1 μM HOE140. Indeed the incorporation rate was even lower in the presence of HOE140, suggesting that it may act as an inverse agonist (*40*). Most interestingly, after ligand stimulation [^{32}P]orthophosphate was exclusively incorporated into the 38 kDa band. It was not incorporated into the 33 kDa protein (Figure 9, right panel), as would be expected for a functional kinin receptor. These findings reinforce our previous conclusion that the minor 38 kDa protein typifies the active B_2 receptor protein in Sf9 cells, whereas the prominent 33 kDa band likely represents a nonfunctional precursor of the B_2 receptor.

The recombinantly expressed B_1 receptor of Sf9 cells showed minor basal phosphorylation in the absence of a ligand, a 1.1 ± 0.2-fold increase of phosphorylation in the presence of desArg[10]kallidin and a 1.3 ± 0.3-fold increase in the presence of desArg[10]kallidin and Leu[9]desArg[10]kallidin. Parallel experiments with [^{35}S]-labeled B_1 receptor demonstrated that sufficient amounts of protein had been immunoprecipitated (cf. Figure 5). Hence the B_1 receptor, unlike the B_2 receptor, does not show a ligand-induced phosphorylation at a significant level. A low basal phosphorylation of B_1 receptor in unstimulated cells likely reflects ligand-independent receptor modification which was not overcome

by Leu^{9}desArg^{10}kallidin. These data signify that the B_1 receptor is not prone to ligand-induced phosphorylation in Sf9 cells, and therefore, it may continue signaling over a sustained period of time, as has been shown for many native cells.

DISCUSSION

Over 80% of all known first messengers, including peptide hormones, bioactive amines, and nucleotides mediate their effects through GPCRs (*41*). Therefore the classification of the corresponding receptors, the cloning of their underlying genes, and the characterization of their cognate proteins has been the very focus of pharmacological research for more than a decade. In particular, attempts have been made to elucidate the roles of post-translational modifications such as phosphorylation, palmitoylation, and/or glycosylation in the desensitization, sequestration, internalization, trafficking, and/or coupling of these receptors (*1*−*3*, *42*). However the characterization of GPCRs at the protein level has proven difficult given their overall hydrophobicity and their low copy numbers in nontransfected cells. In this situation, the baculovirus system has been utilized to overcome the paucity of GPCR proteins (*4*, *8*−*13*, *37*, *43*). Potential shortcomings of the system include, for example, the production of truncated GPCRs (*9*, *37*) and the problems associated with the measurement of secondary messengers such as inositol-1,4,5-trisphosphate (*37*). Here we have set out to study a prototypic class of hormone GPCRs, the kinin receptors produced by Sf9 cells, and sought to characterize the receptors with respect to their structure and function.

Kinin receptors heterologously expressed by Sf9 cells display the same ligand profiles as have been reported for endogenous kinin receptors and kinin receptors overexpressed in mammalian cells (*26*, *27*, *31*, *32*, *44*). The expression level of B_2 receptor (∼2000 fmol/mg) was similar to that reported for CHO cells (*44*), while that for the B_1 receptors (∼150 fmol/mg) was among the highest reported so far (*28*, *36*, *45*). Overexpression of the B_1 receptor in Sf9 cells and the production of specific antipeptide antibodies have enabled us to demonstrate that the B_1 receptor is a protein of 30 kDa in Sf9 cells. We anticipate that the relative molecular mass of the B_1 receptor may considerably diverge when expressed in higher eucaryotic cells as we have observed for the B_2 receptor. More importantly we have been able to demonstrate in Sf9 cells that, unlike B_2, the B_1 receptor fails to undergo significant ligand-induced phosphorylation. This finding may help explain the long-observed failure of the B_1 receptor to desensitize in response to its cognate agonist in many other cells (*28*, *29*). Due to technical limitations, that is, poor adherence of Sf9 cells in the fura assay and insufficient loading of Sf9 cells with [^{3}H]inositol in the IP_3 assay, we have been unable to directly follow desensitization of the B_1 receptor in these cells. Also we have not addressed alternative B_1 receptor desensitization mechanisms such as internalization (*8*, *46*). Further studies taking advantage of the availability of B_1/B_2 receptor chimeras (*46*), combined with a site-directed mutagenesis approach, should allow to pinpoint the structural elements that confer the deviant desensitization kinetics of kinin receptors.

The disparity of desensitization mechanisms for the two kinin receptor subtypes does not come as surprise. Indeed previous studies have disclosed that the kinin receptors markedly differ by other features such as (i) their expression patterns, that is, the expression of the B_1 gene is inducable by cytokines whereas the B_2 receptor gene is constitutively expressed; (ii) their exquisitely distinct ligand specificity, that is, almost all known B_2 ligands convert into B_1 ligands by the selective removal of a carboxy-terminal arginine residue; and (iii) their tissue distribution (*26*, *27*).

The development of specific antibodies to the kinin receptors highlights a few facets of these peculiar proteins, that is, epitope propensity, antigen responsiveness, and self-association. Among the many antisera that we have generated, those directed to the carboxy-terminal domains of both kinin receptors are outstanding in both their specificity and their performance. This propensity may reflect differential segmental flexibility, hydrophilicity, and/or accessibility of the carboxy-terminal receptor domain. Indeed the most efficient monoclonal antibody generated to the B_2 receptor recognizes the same target epitope, that is, intracellular domain ID4 (Micke, Blaukat, and Müller-Esterl, unpublished experiments). Titration of the minimum amount of receptor protein detectable by antibodies to ID4 indicated that ≥4 ng of B_2 fusion protein corresponding to 120 fmol of B_2 receptor/lane is required for successful Western blotting. This figure translates into a minimum expression level of 1.2 pmol of receptor/mg of cellular protein (assuming that 100 μg of total protein is loaded per lane) to allow reliable detection of the B_2 receptor in crude lysates. Finally our immunoprecipitation experiments with anti-ID4 may hint to a selective oligomerization of the functional form of the B_2 receptor of 38 kDa but not of the nonfunctional 33 kDa precursor. Indeed the dimerization of GPCRs has been implicated in the regulation of receptor activity (*47*−*50*). We have not further addressed whether B_2 receptor multimerization occurs under physiological conditions, or whether it is only an artifact of our solubilization procedure.

An unexpected finding of this study is the dramatic imbalance between the total number of receptor proteins and the cognate ligand-binding sites. Our studies with the B_2 receptor promote the notion that a nonfunctional precursor of 33 kDa predates the "mature" 38 kDa protein. The former protein is not glycosylated, whereas the latter is. We are unaware of a precedent where glycosylation confers functional activity to a GPCR. The distinct possibility remains that the 33 kDa form is inaccessible to the ligand due to its location in intracellular compartments and, therefore, accounts for the observed effects. We have not attempted to gain binding capacity by denaturation/refolding procedures or by detergent treatment (*1*) of the 33 kDa protein. The fact that the imbalance between protein- and ligand-binding sites was even more pronounced for the B_1 receptor clearly warrants further studies to discriminate between these possibilities. Indeed observations made in COS-7 cells during transient overexpression of B_2 receptor as well as in HF-15 fibroblasts with endogenous B_2 receptor (Blaukat and Müller-Esterl, unpublished experiments) suggest that glycosylation and insertion of receptors into the plasma membrane are limiting steps in the expression of functional GPCRs for many different cell types.

Regardless of its functional state, the prominent B_2 protein of 33 kDa has proven a valuable asset of the Sf9 system. It has allowed isolating, by a single immunoaffinity chromatography step, significant quantities of the apparently ho-

mogeneous receptor. This receptor preparation has been subsequently used for the screening of hybridoma cells for monoclonal antibodies to the receptor; it also has been utilized in an enzyme-linked immunosorbent assay-based screen for autoantibodies to the B_2 receptor in patients' plasma (Micke and Müller-Esterl, unpublished experiments). We anticipate that the bulk production of GPCRs by the baculovirus system will aid in solving some of the conundrums of heptahelical receptor research, that is, the precise structural definition of a ligand-binding site for oligopeptidic ligands, the isolation of unique receptor states, and, above all, the elucidation of the three-dimensional structure of a G protein-coupled receptor at high resolution.

ACKNOWLEDGMENT

The authors wish to thank B. Welsch and Drs. A. Maidhof (Mainz, Germany) for the production of antisera, F. Hess (West Point, PA) for the human B_1 receptor cDNA and a reference antibody to this receptor, A. Horstmeyer (Berlin, Germany) for valuable help in the early phase of this study, and D. Kyle (Sunnyvale, CA) and I. Dikic (Uppsala, Sweden) for support.

REFERENCES

1. Couvineau, A., Fabre, C., Gaudin, P., Maoret, J.-J., and Laburthe, M. (1996) *Biochemistry 35*, 1745−1752.
2. Bouvier, M., Loisel, T. P., and Hebert, T. (1995) *Biochem. Soc. Trans. 23*, 577−581.
3. Lohse, M. J. (1993) *Biochim. Biophys. Acta 1179*, 171−188.
4. Loisel, T. P., Ansanay, H., St-Onge, S., Gay, B., Boulanger, P., Strosberg, D., Marullo, S., and Bouvier, M. (1997) *Nat. Biotechnol. 15*, 1300−1304.
5. Shetzline, M. A., Premont, R. T., Walker, J. K. L., Vigna, S. R., and Caron, M. G. (1998) *J. Biol. Chem. 273*, 6756−6762.
6. Diviani, D., Lattion, A. L., and Cotecchia, S. (1997) *J. Biol. Chem. 272*, 28712−28719.
7. Tobin, A. B., and Nahorski, S. R. (1993) *J. Biol. Chem. 268*, 5542−5549.
8. Cramer, H., Müller-Esterl, W., and Schroeder, C. (1997) *Biochemistry 36*, 13325−13332.
9. Grünewald, S., Reiländer, H., and Michel, H. (1996) *Biochemistry 35*, 15162−15173.
10. Kwatra, M. M., Schreurs, J., Schwinn, D. A., Innis, M. A., Caron, M. G., and Lefkowitz, R. J. (1995) *Protein Expression Purif. 6*, 717−721.
11. Pei, G., Tiberi, M., Caron, M. G., and Lefkowitz, R. J. (1994) *Proc. Natl. Acad. Sci. U.S.A. 91*, 3633−3636.
12. Richardson, R. M., and Hosey, M. M. (1992) *J. Biol. Chem. 267*, 22249−22255.
13. Parker, E. M., Kameyama, K., Higashijima, T., and Ross, E. M. (1991) *J. Biol. Chem. 266*, 519−527.
14. Reiländer, H., Boege, F., Vasudevan, S., Maul, G., Hekman, M., Dees, C., Hampe, W., Helmreich, E. J. M., and Michel, H. (1991) *FEBS Lett. 282*, 441−444.
15. Gimpl, G., Anders, J., Thiele, C., and Fahrenholz, F. (1996) *Eur. J. Biochem. 237*, 768−777.
16. Quehenberger, O., Prossnitz, E. R., Cochrane, C. G., and Ye, R. D. (1992) *J. Biol. Chem. 267*, 19757−19760.
17. Bhoola, K. D., Figueroa, C. D., and Worthy, K. (1992) *Pharmacol. Rev. 44*, 1−80.
18. Regoli, D., and Barabé, J. (1988) *Methods Enzymol. 163*, 210−230.
19. Liebmann, C., Graness, A., Ludwig, B., Adomeit, A., Boehmer, A., Boehmer, F. D., Nürnberg, B., and Wetzger, R. (1996) *Biochem. J. 313*, 109−118.
20. Wilk-Blaszczak, M. A., Singer, W. D., Gutowski, S., Sternweis, P. C., and Belardetti, F. (1994) *Neuron 13*, 1215−1224.
21. Liebmann, C., Mammery, K., and Graness, A. (1994) *Eur. J. Pharmacol. 288*, 35−43.
22. Gutowski, S., Smrcka, A., Nowak, L., Wu, D. G., Simon, M., and Sternweis, P. C. (1991) *J. Biol. Chem. 266*, 20519−20524.
23. Burch, R. M., and Axelrod, J. (1987) *Proc. Natl. Acad. Sci. U.S.A. 84*, 6374−6378.
24. Tippmer, S., Quitterer, U., Kolm, V., Faussner, A., Roscher, A. A., Müller-Esterl, W., and Häring, H. (1994) *Eur. J. Biochem. 225*, 297−304.
25. Palmer, R. M., Ferrige, A. G., and Moncada, S. (1987) *Nature 327*, 524−526.
26. Marceau, F. (1995) *Immunopharmacology 30*, 1−26.
27. Hall, J. M. (1992) *Pharmacol. Ther. 56*, 131−190.
28. Austin, C. E., Faussner, A., Robinson, H. E., Chakravarty, S., Kyle, D. J., Bathon, J. M., and Proud, D. (1997) *J. Biol. Chem. 272*, 11420−11425.
29. Mathis, S. A., Criscimagna, N. L., and Leeb-Lundberg, L. M. F. (1996) *Mol. Pharmacol. 50*, 128−139.
30. Hock, F. J., Wirth, K., Albus, U., Linz, W., Gerhards, H. J., Wiemer, G., Henke, S., Breipohl, G., König, W., Knolle, J., and Schölkens, B. A. (1991) *Br. J. Pharmacol. 102*, 769−773.
31. Menke, J. G., Borkowski, J. A., Bierilo, K. K., MacNiel, T., Derrick, A. W., Schneck, K. A., Ransom, R. W., Strader, C. D., Linemeyer, D. L., and Hess, J. F. (1994) *J. Biol. Chem 269*, 21583−21586.
32. Hess, J. F., Borkowski, J. A., Young, G. S., Strader, C. D., and Ransom, R. W. (1992) *Biochem. Biophys. Res. Commun. 184*, 260−268.
33. Blaukat, A., Abd Alla, S., Lohse, M. J., and Müller-Esterl W. (1996) *J. Biol. Chem. 271*, 32366−32374.
34. Abd Alla, S., Buschko, J., Quitterer, U., Maidhof, A., Haasemann, M., Breipohl, G., Knolle, J., and Müller-Esterl, W. (1993) *J. Biol. Chem. 268*, 17277−17285.
35. Abd Alla, S., Quitterer, U., Grigoriev, S., Maidhof, A., Haasemann, M., Jarnagin, K., and Müller-Esterl, W. (1996) *J. Biol. Chem. 271*, 1748−1755.
36. Hess, J. F., Derrick, A. W., MacNeil, T., and Borkowski, J. A. (1996) *Immunopharmacology 33*, 1−8.
37. Horstmeyer, A., Cramer, H., Sauer, T., Müller-Esterl, W., and Schroeder, C. (1996) *J. Biol. Chem. 271*, 20811−20819.
38. Herzig, M. S. C., and Leeb-Lundberg, L. M. F. (1995) *J. Biol. Chem. 270*, 20591−20598.
39. Yaqoob, M., and Snell, C. R. (1994) *J. Neurochem. 62*, 17−26.
40. Chidiac, P., Hebert, T. E., Valiquette, M., Dennis, M., and Bouvier, M. (1994) *Mol. Pharmacol. 45*, 490−499.
41. Birnbaumer, L., and Brown, A. M. (1990) *Am. Rev. Respir. Dis. 141*, 106−114.
42. Böhm, S. K., Grady, E. F., and Bunnett, N. W. (1997) *Biochem. J. 322*, 1−18.
43. Kwatra, M. M., Schwinn, D. A., Schreurs, J., Blank, J. K., Kim, C. M., Benovic, J. L., Krause, J. E., Caron, M. G., and Lefkowitz, R. J. (1993) *J. Biol. Chem. 268*, 9161−9164.
44. Pizard, A., Marchetti, J., Allegrini, J., Alhenc-Gelas, F., and Rajerison, R. M. (1998) *J. Biol. Chem. 273*, 1309−1315.
45. Bastian, S., Loillier, B., Paquet, J. L., and Pruneau, D. (1997) *Br. J. Pharmacol. 122*, 393−399.
46. Faussner, A., Proud, D., Towns, M., and Bathon, J. M. (1998) *J. Biol. Chem. 273*, 2617−2623.
47. Hebert, T., Moffet, S., Morello, J. P., Loisel, T. P., Bichet, D. G., Barret, C., and Bouvier, M. (1996) *J. Biol. Chem. 271*, 16394−16392.
48. Hebert, T., Loisel, T. P., Adam, L., Ethier, N., St-Onge, S., and Bouvier, M. (1998) *Biochem. J. 330*, 287−293.
49. Monnot, C., Bihoreau, C., Conchon, C., Curnow, K. M., Corvol, P., and Clauser, E. (1996) *J. Biol. Chem. 271*, 1507−1513.
50. Maggio, R., Vogel, Z., and Wess, J. (1993) *Proc. Natl. Acad. Sci. U.S.A. 90*, 3103−3107.

BI981727R